Journal of Environmental Radioactivity 150 (2015) 132–144

Contents lists available at ScienceDirect

Journal of Environmental Radioactivity

journal homepage: www.elsevier.com/locate/jenvrad

Dose rate estimates and spatial interpolation maps of outdoor gamma dose rate with geostatistical methods; A case study from Artvin, Turkey

Cafer Mert Yeşilkanat [a, *], Yaşar Kobya [b], Halim Taşkin [c], Uğur Çevik [d]

[a] Artvin Çoruh University, Faculty of Art and Science, Department of Physics, 08100 Artvin, Turkey
[b] Artvin Çoruh University, Faculty of Engineering, Energy Systems Engineering, 08100 Artvin, Turkey
[c] TAEK, Cekmece Nuclear Research and Training Centre, Altınşehir Yolu 5 Km, Halkali, 34303 Istanbul, Turkey
[d] Karadeniz Technical University, Faculty of Science, Department of Physics, 61000 Trabzon, Turkey

ARTICLE INFO

Article history:
Received 27 March 2015
Received in revised form
18 August 2015
Accepted 18 August 2015
Available online 29 August 2015

Keywords:
Dose estimation
Outdoor gamma dose rate
Interpolated map
Geostatistic
Artvin

ABSTRACT

In this study, compliance of geostatistical estimation methods is compared to ensure investigation and imaging natural Fon radiation using the minimum number of data. Artvin province, which has a quite hilly terrain and wide variety of soil and located in the north–east of Turkey, is selected as the study area. Outdoor gamma dose rate (OGDR), which is an important determinant of environmental radioactivity level, is measured in 204 stations. Spatial structure of OGDR is determined by anisotropic, isotropic and residual variograms. Ordinary kriging (OK) and universal kriging (UK) interpolation estimations were calculated with the help of model parameters obtained from these variograms. In OK, although calculations are made based on positions of points where samples are taken, in the UK technique, general soil groups and altitude values directly affecting OGDR are included in the calculations. When two methods are evaluated based on their performances, it has been determined that UK model ($r = 0.88$, $p < 0.001$) gives quite better results than OK model ($r = 0.64$, $p < 0.001$). In addition, as a result of the maps created at the end of the study, it was illustrated that local changes are better reflected by UK method compared to OK method and its error variance is found to be lower.

1. Introduction

We can talk about two types of radiation in the nature as natural and artificial radiation. The largest contribution to natural radiation is made by cosmic and terrestrial sources, which are ionizing radiation types, after radon (Rafique et al., 2014). Cosmic gamma radiation is caused from outside of the earth's atmosphere and causes 50% of the annual dose (Hiemstra et al., 2009). In addition, the degree of cosmic gamma radiation varies depending on solar activity, altitude (Quarto et al., 2013), atmospheric pressure (Hiemstra et al., 2009). Terrestrial gamma radiation sources are caused by radioactive nuclei that exist in the soil and varies depending on geological structure and soil type (Norbani et al., 2014; Taskin et al., 2009). The artificial radiations in the nature are caused by nuclear weapons tests, nuclear reactor fall-outs and medical works. Outdoor gamma dose rate is an important determinant comes from above-mentioned natural and artificial sources and determines the level of radioactivity in a media.

Identifying and monitoring artificial and natural radioactivity levels of habitats is very important in terms of public health (UNSCEAR, 2000). It is known that outdoor gamma dose rates have a positive relationship with malignant tumors (Tondel et al., 2011). Therefore, since certain levels of outdoor gamma dose rates pose a potential threat to human health, it is necessary to determine and monitor the level of outdoor gamma dose rate especially in densely populated areas. In the last decade, several studies were carried out to assess the average outdoor terrestrial gamma dose rate in air (Baykara and Doğru, 2009; Karahan and Bayulken, 2000; Norbani et al., 2014; Quarto et al., 2013; Taskin et al., 2009; UNSCEAR, 2000).

Determination of environmental radioactivity is a time consuming and costly process. For this reason, the area to be studied should be well-chosen while creating radiological Fon

* Corresponding author.
E-mail address: cmertyesilkanat@gmail.com (C.M. Yeşilkanat).

http://dx.doi.org/10.1016/j.jenvrad.2015.08.011
0265-931X/

maps. These maps should represent the area with minimum amount of data to save time and minimize the costs (EUR 21595 EN, 2005). In addition, estimation values for interpolation regions, where no measurement are made, should also be calculated with the help of the regions, where measurements are made, and results should be compared with cross-validation. Geostatistics is a quite useful method to be used to characterize and map this spatial variability (Dai et al., 2007). In recent years, geostatistics is used to explain spatial correlation by many authors (Charro et al., 2013; Hiemstra et al., 2009; McGrath et al., 2004; Norbani et al., 2014; Pebesma, 2005; Sanusi et al., 2014; Savelieva, 2005).

The aim of this study is determining the most appropriate method in order to estimate and map the radioactivity levels of (Outdoor gamma dose) a region within the shortest time with minimum cost by representing the study area with minimum amount of sample. In addition, the necessary procedure to map the radioactivity Fon map is explained geostatistically in this study.

2. Materials and methods

2.1. Study area

The province of Artvin is situated in the most north–east of Turkey between the latitudes of 40° 36′ and 41° 31′ N and the longitudes of 41° 09′ and 42° 35′ E (Fig. 1). It covers approximately 1% of the country with an areameter of 7436 km^2 and according to the 2014 data, the population of the region is 169,334 among which the populations of the rural parts and the cities are 94,316 and 75,018, respectively (Statistic Department of Turkey, 2014). Topographic structure of the region is rough, altitudes ranging from 0 m to 3000 m are present. Fig. 2 shows the digital evelation map of the region. The increase in the quantity of cosmic rays causes the gamma dose rates to be higher (Mishev and Hristova, 2012; O'Brien et al., 1996).

2.2. Geological properties and soil types of study area

Considering the geological properties of the region, Middle-Upper Eocean, Upper Cretaceous and Lower middle Jurassic volcanites and sediments, Upper Cretaceous dacite rhyolite rhyodacide, Pleocene-Eocene and upper Pleozoic Granitoid rocks are dominating the area (Ustaomer et al., 2012). Fig. 3 shows the geological structure and rock structure of the study area. Terrestrial gamma dose rate that forms 50% of the outer gamma dose rates depends on 0–30 cm deep rock structure and geological elements. High radiation levels are especially seen in volcanoclastic rocks as; granite, cyanite, gabbro and pyrites. Such rock structures are substantial ^{238}U, ^{232}Th, ^{40}K resources and are the structures that were crystallized under high pressure, and high temperature (Chiozzi et al., 2002). The relationship between geological structure and dose rates has been studied by many researchers (Norbani et al., 2014; Otansev et al., 2012; Sanusi et al., 2014).

The soil spreading over Artvin area can be studied under six groups; red – yellow podzolic soils (P) (17%), high mountain meadow soils (Y) (17%), non-calcic brown forest soils (N) (12%), alluvial (A) (4%), Collivial (C) (2%), brown forest soils (M) (%48) (Yuksek and Ölmez, 2002). These are shown in Fig. 4. Among these soil types, especially brown forest soils and non-calcic brown forest soils cause high levels of radiation because of U-238 and Th-232 they include (Degerlier et al., 2008). Moreover, soils in Artvin are rich in organic materials since there is not enough weathering and decomposition of organic materials in the region. There is a positive relationship between organic materials in soil and radioactivity level (Ramasamy et al., 2014).

2.3. Outdoor gamma dose rate determination

In order to determine the outdoor gamma dose rates, the study area was separated to 204 sampling stations with approximately

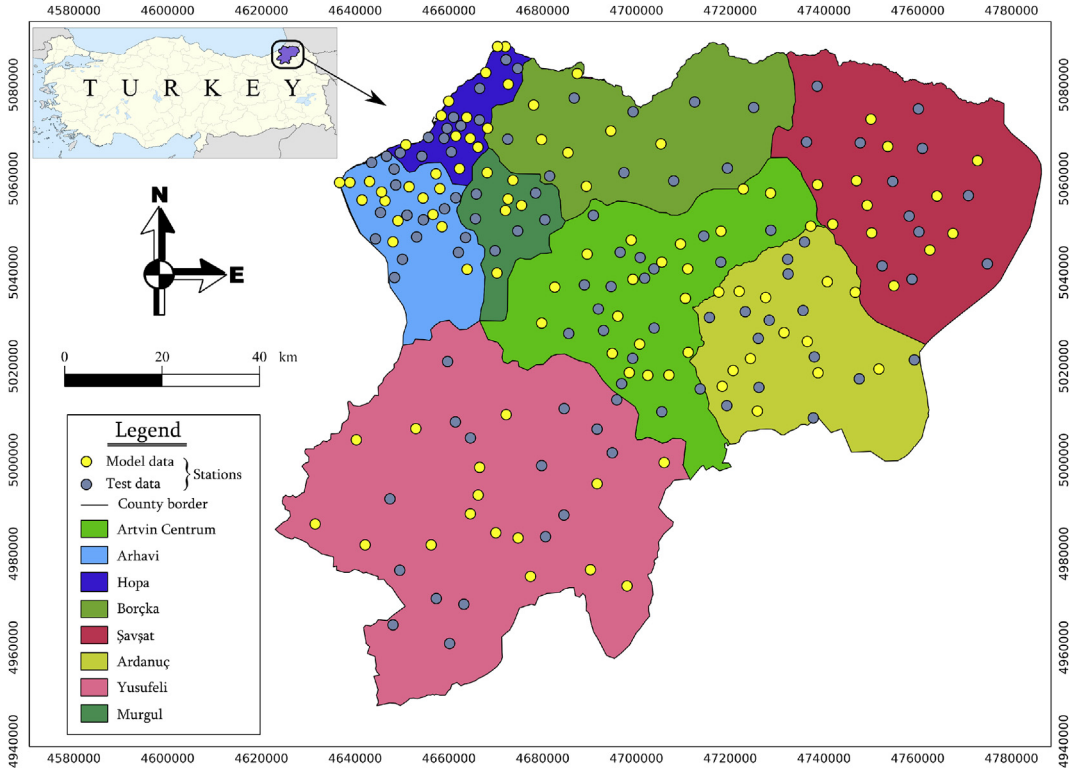

Fig. 1. Study area and the places where samples were taken.

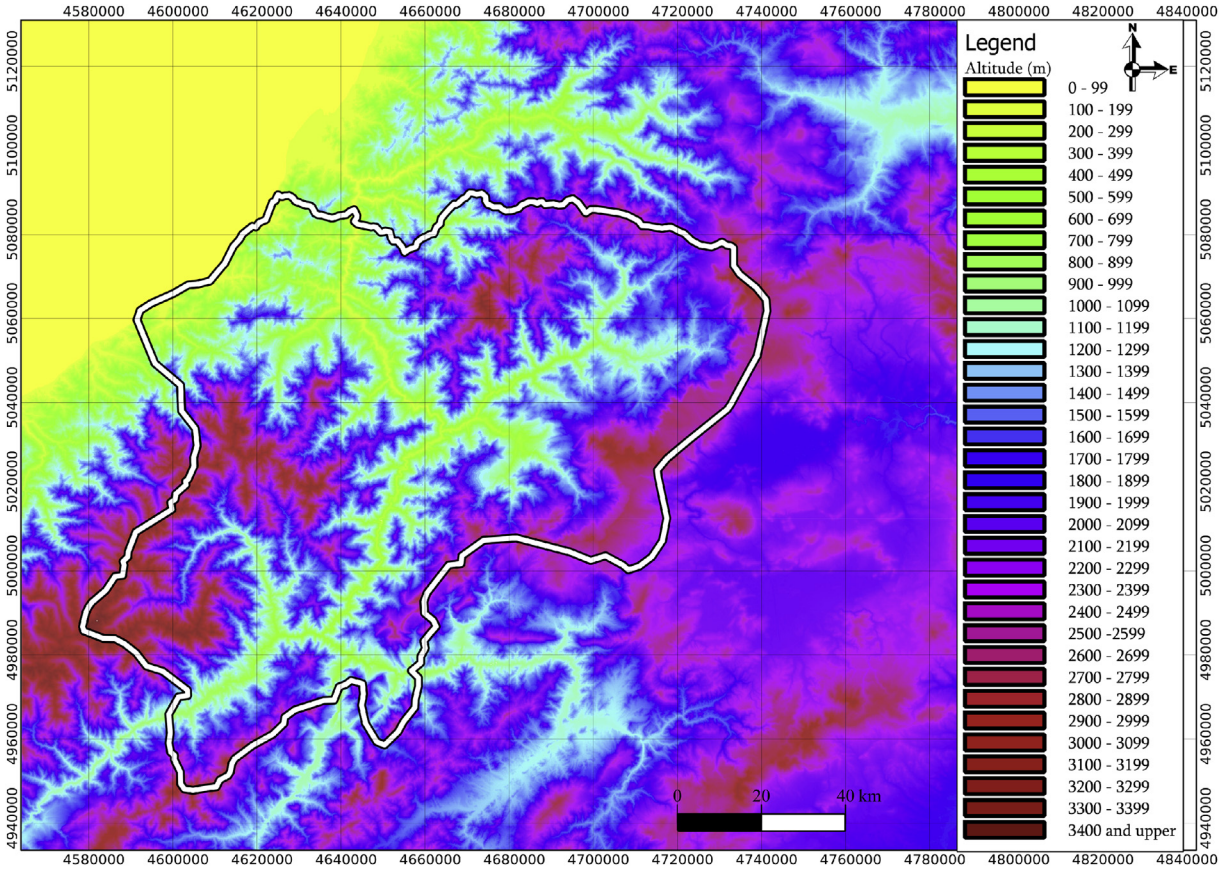

Fig. 2. Altitude map for Artvin that was specified by digital elevation model (USGS, 2013).

3 km distance. Measurings were done in 3 different locations for each sampling station (Kobya et al., 2015). The average of these 3 measurements was taken and was specified as outdoor gamma dose rate for sampling stations (Fig. 1). 50% (102) of the stations were randomly reserved for modelling and 50% (102) were reserved for validation test. The outdoor gamma dose rates were measured by Eberline smart portable device (ESP-2) connected with an SPA-6 model plastic scintillation detector. Measurements were taken in air for two minutes at 1 m above the ground and the gamma dose rates were recorded as μSv h^{-1} and then converted to nGy h^{-1} (Taskin et al., 2009). (1 μSv/h = 1000 nGy/h = 100 μR/h).

Fig. 5a and b shows histograms and summary statistics for model and test data, respectively. In this way, Kolmogorov–Smirnov test (D = 0.2, p-value = 0.99) shows that both histograms are not so different from each other. So, both model data and the test data have the same statistical structure. Furthermore; with Shapiro–Wilk normality test ($p < 0.05$), the two data set were seen not to have normal distribution. In order to get rid of this situation which breaks the structure of variogram and causes kriging weighties to be calculated wrong, the distribution should be converted to normal distribution.

2.4. Geostatistical analysis

Geostatistics is a statistical calculation method whose basis depends on the theory of stable coincidence in theory of functions and which deals with the relationships of samples by considering the coordinates the samples were taken unlike conventional statistical methods. This calculation method has significant advantages as; determining the amount of errors in certain confidence level (Clark, 1979). In geostatistics, the change in the spatial variables depending on the distance is specified with variogram or semivariogram function and this function is defined as the variance of the variables which are as distant from each other as *h*. The increase in variance can be interpreted as decrease in the relationship. In other words, the size of variance between two points depends on the size of distance between them (Diggle and Riberioj, 2007). Semivariance for the whole space measured can be defined with the equation below;

$$V(h) = \frac{1}{2N(h)} \sum_{i=1}^{N(h)} (Z(x_i) - Z(x_i + h))^2 \quad (1)$$

Here, $V(h)$ is semivariance value, h is the distance between two points, $N(h)$ is the number of point couples in h distance (or the number of h vector in the sturdy area), $Z(x_i)$ is the measured value of the variable in i point, $Z(x_i + h)$ is the measured value of the variable in $x_i + h$ point. This experimental semivariogram function is calculated for each measurement pair and for each direction and then an appropriate parametric function is fitted. The most used models in the literature are; spherical (Eq. (2)), exponential (Eq. (3)), gauss (Eq. (4)), pentaspherical (Eq. (5)), linear (Eq. (6)) ve circular (Eq. (7)) (Webster and Oliver, 2007).

$$V(h) = \begin{cases} c_0 + c\left(\frac{3h}{2a} - \frac{1}{2}\left(\frac{h}{a}\right)^3\right) & \text{for } h \le a, \\ c_0 + c & \text{for } h > a. \end{cases} \quad (2)$$

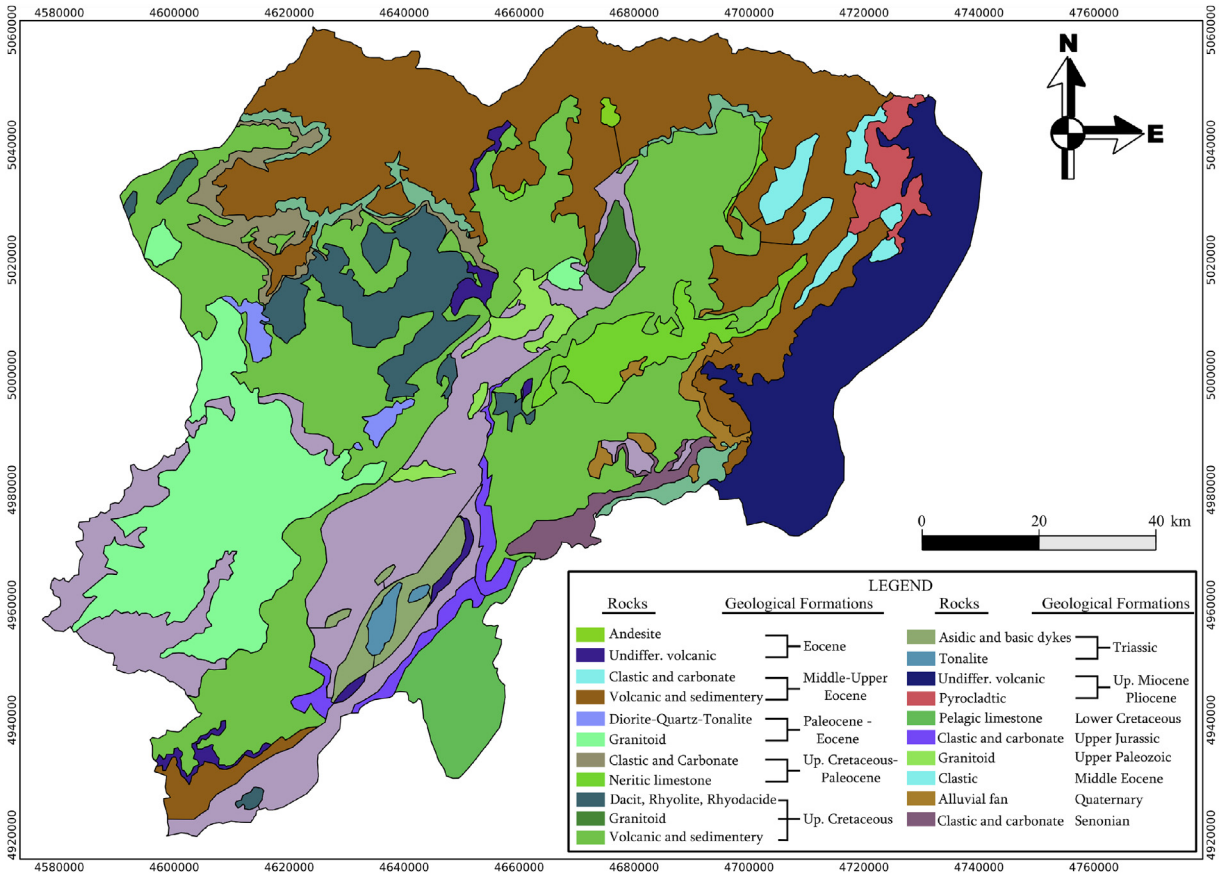

Fig. 3. Geological map of Artvin (MTA, 2002).

$$V(h) = c_0 + c\left(1 - \exp\left(-\frac{h}{r}\right)\right), \quad \text{for h} \geq 0 \tag{3}$$

$$V(h) = c_0 + c\left(1 - \exp\left(-\frac{h^2}{r^2}\right)\right), \quad \text{for h} \geq 0 \tag{4}$$

$$V(h) = \begin{cases} c_0 + c\left(\dfrac{15h}{8a} - \dfrac{5}{4}\left(\dfrac{h}{a}\right)^3 + \dfrac{3}{8}\left(\dfrac{h}{a}\right)^5\right) & \text{for} \quad \text{h} \leq \text{a}, \\ c_0 + c & \text{for} \quad \text{h} > \text{a}. \end{cases} \tag{5}$$

$$V(h) = \begin{cases} c_0 + c\left(\dfrac{h}{a}\right) & \text{for} \quad \text{h} \leq \text{a}, \\ c_0 + c & \text{for} \quad \text{h} > \text{a}. \end{cases} \tag{6}$$

$$V(h) = \begin{cases} c_0 + c\left(1 - \dfrac{2}{\pi}\cos^{-1}\left(\dfrac{h}{a}\right) + \dfrac{2h}{\pi a}\sqrt{1 - \dfrac{h^2}{a^2}}\right) & \text{for} \quad \text{h} \leq \text{a}, \\ c_0 + c & \text{for} \quad \text{h} > \text{a}. \end{cases} \tag{7}$$

where a is the range; i.e. separation at which there is no more spatial depence, c is the sill: i.e. maximum semivariance, c_0 is Nugget effect: that is to say; the part representing the homogeneity of the study area and h is lag distance. The fitted model provides the necessary input parameters for kriging interpolation. In addition, it gives information about the spatial structure of the region. Cross-validation process was done for finding the right model. In cross-validation, an observation point is excluded from data set and this point is estimated by applying kriging model that is formed by using the other points. Standard errors of the estimations for excluded points are calculated and three supplementary statistics are applied. These are; mean error, ME (Eq. (8)), root mean squared error, RMSE (Eq. (9)) and mean squared deviation ratio, MSDR (Eq. (10)). Since kriging is an unbiased method, ME should be "0" ideally. Since kriging is callous towards the errors in semivariogram, the calculated ME is a weak supplement. RMSE is entailed to be small (approximately "0"). If the semivariogram model is true, RMSE should be equal to the square of kriging variation. For this reason, MSDR should be "1" (Webster and Oliver, 2007).

$$ME = \frac{1}{N}\sum_{i=1}^{N}\left\{Z(x_i) - \widehat{Z}(x_i)\right\} \tag{8}$$

$$RMSE = \sqrt{\frac{1}{N}\sum_{i=1}^{N}\left[Z(x_i) - \widehat{Z}(x_i)\right]^2} \tag{9}$$

$$MSDR = \frac{1}{N}\sum_{i=1}^{N}\frac{\left[Z(x_i) - \widehat{Z}(x_i)\right]^2}{\widehat{\sigma}^2(x_i)} \tag{10}$$

Here, $\widehat{\sigma}^2(x_i)$ is kriging variance in x_i point, $Z(x_i)$ is the known value, $\widehat{Z}(x_i)$ is the estimated value and N is the data number. The basic method of geostatistics, kriging method is used in the study.

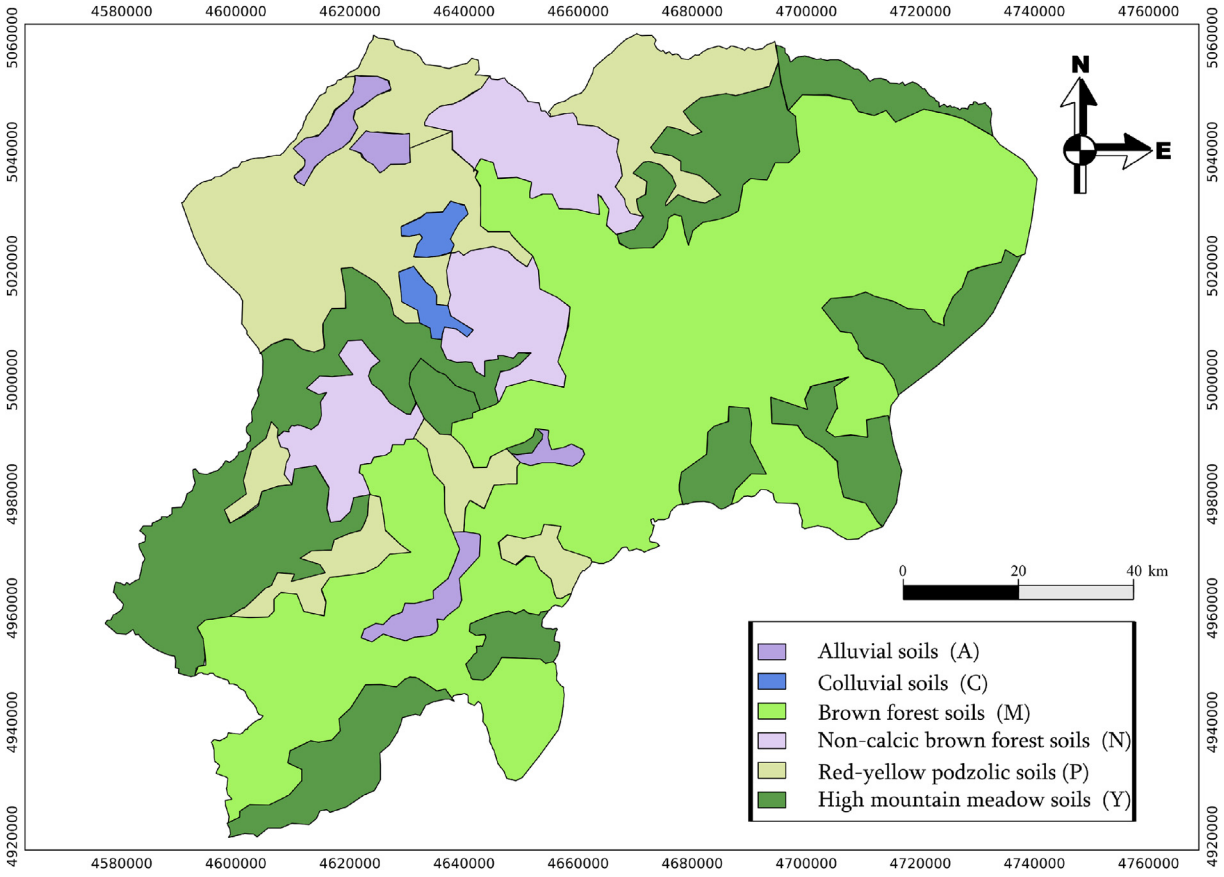

Fig. 4. Great soil group map of Artvin (Yavuz Özalp et al., 2013).

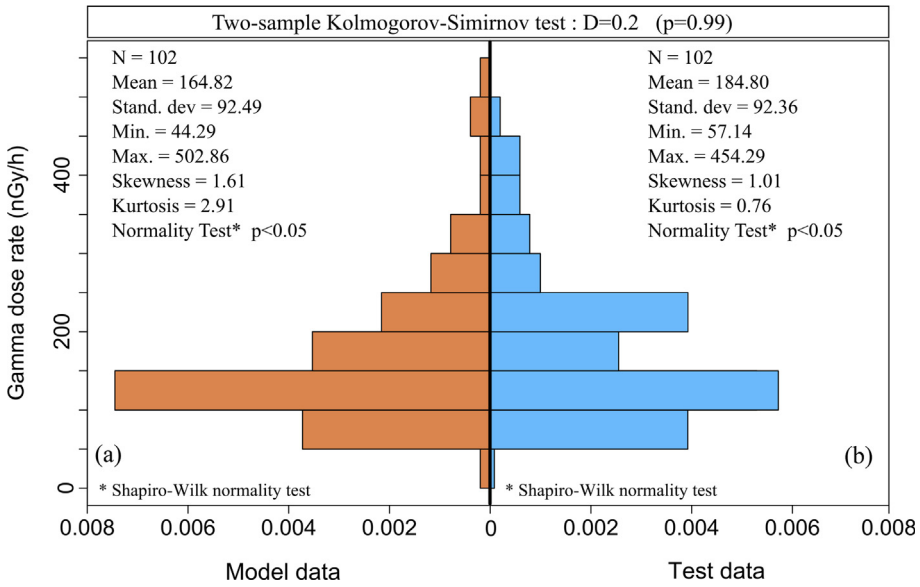

Fig. 5. The histogram and descriptive statistics of (a) model data and (b) test data.

This method is defined as the BLUE (best linear unbiased estimator) mathematically (Boogaart and Schaeben, 2002). That means the identification of weight according to the condition that estimated errors are minimum. Kriging method uses a weight model that ensures more response to nearby points as in the method of weighted mean in conventional statistics theorem (McGrath et al., 2004). In the recent years, researchers have studies many kriging methods as; Simple kriging (Li et al., 2009), Ordinary kriging (Alvarez-Gallego et al., 2015; Elbasiouny et al., 2014; Sanusi et al., 2014), universal kriging (Cafaro et al., 2014; Hiemstra et al., 2009), cokriging (Lark et al., 2014; Warnery et al., 2015) and indicator kriging (Chica-Olmo et al., 2014). The most common two

methods; ordinary and universal kriging were used for this study.

The general equation of kriging method;

$$Z(x_0) = \sum_{i=1}^{N} W_i Z(x_i) \tag{11}$$

Here $Z(x_0)$ is unknown but estimated Z value in x_0 point, W_i is weight value for each $Z(x_i)$ which are used for the calculation of $Z(x_0)$, experimental data that are used to estimate $Z(x_i)$ and $Z(x_0)$, N is the point number used for calculating $Z(x_0)$. As in conventional statistics, a normal distribution for the variable under study is desirable in linear geostatistics (Clark and Harper, 2000). In geostatistical analysis, abnormality in the distribution breaks the structure of the variogram and causes wrong calculations. So, data conversions were applied in order to enable usually log-normal experimental data to fit for normal distribution (Krige, 1966; McGrath et al., 2004). In Fig. 6, the histograms of log-transformed data both for data set and the model set are given. The two histograms are not seen to be significantly different from each other with Kolmogorov–Smirnov test (D = 0.1, p-value = 0.99). Moreover, the two data set was determined to be possessing normal distribution ($p > 0.05$) with Shapiro–Wilk normality test.

2.4.1. Ordinary kriging (OK)

In OK method, the average of spatial random field $[Z(x)]$ is assumed to be stationary (Armstrong, 1998) and this is named as unbiasedness. OK estimation is given in Eq. (11). In order to make and unbiased equation, the mean of estimated errors should meet the requirements of $E[Z(x_i) - Z(x_0)] = 0$ and the mean of estimation errors should meet the requirements of $Var[Z(x_i) - Z(x_0)] = Min$. Here, in order to make an unbiased interpolation, it is necessary for the total weight to be equal to $1(\sum_{n=i}^{N} W_i = 1)$ (Armstrong, 1998).

2.4.2. Universal kriging (UK)

In cases where regional variables are not stationary, trends may occur in certain areas. In this case, components of this trend should be used in UK calculations as an additional data. In this situation, as given in Eq. (12) spatial random field $[Z(x_0)]$ is written as the trend component and the total of error terms (Hiemstra et al., 2009).

$$Z(x_0) = W_0 + \sum_{i=1}^{N} W_i f_i(x) + e(x) \tag{12}$$

Here, W_0 and W_i are unknown regression parameters, $f_i(x)$ is the i-th known predictor at location, x is a function that changes according to the structure of the area and defines trend and $e(x)$ is error term. The average of this error term is 0, covariance between $e(x)$ and $e(x+h)$ is identified with only h distance vector (Chilès and Delfiner, 1999; Deutsch and Journel, 1998). In this study, the two factors; altitude and soil type that directly affect gamma dose rates as estimators are used in universal kriging method.

2.5. Software resources and mapping

All the analyses are carried out in the R environment for statistical computing and visualisation (Ihaka and Gentleman, 1996; R Development Core Team, 2005) and the gstat (Pebesma and Wesseling, 1998), sp (Pebesma and Bivand, 2005) R packages which is an open-source dialect of the S statistical computing language. It is free, runs on most computing platforms, and contains contributions from top computational statisticians. Maps are formed by Quantum geographic information system (QGIS) vs 1.8.0 (Quantum GIS Development Team, 2014). All interpolation and simulation maps are in the size of 100 × 100 m^2 pixels (1 ha spatial resolution).

3. Results and discussion

3.1. The factors affecting gamma dose

In order for gamma dose rates to be estimated best, the relationship between two factors that directly affect these dose

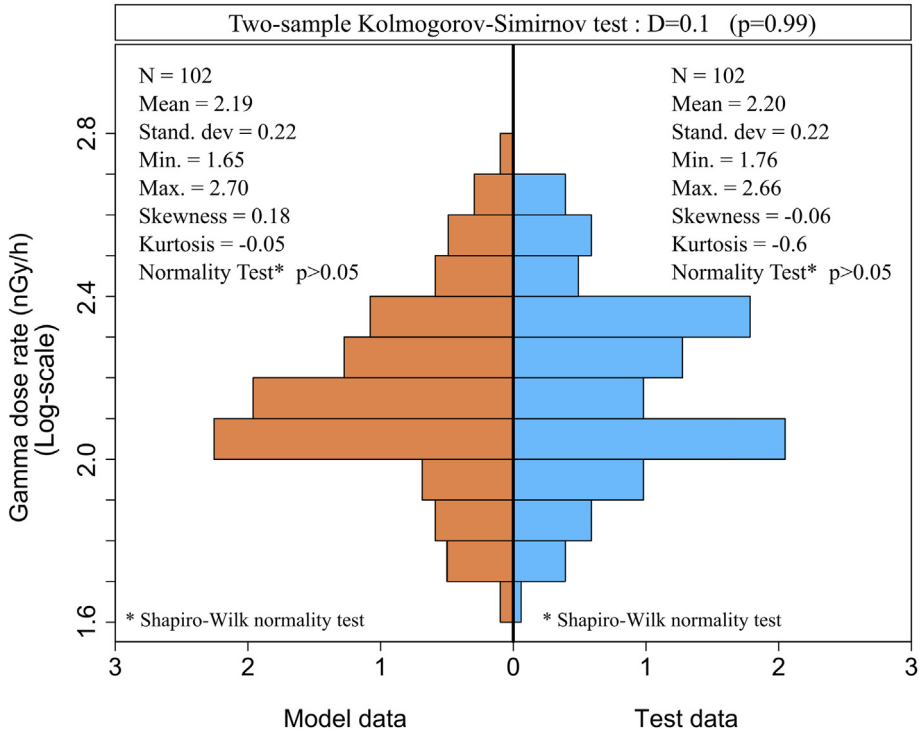

Fig. 6. The histogram and descriptive of model and log-transformed data.

rates; elevation and soil type is studied. There is a significant positive correlation ($r = 0.880$, $p < 0.001$, $n = 102$; for model data) found between the first factor, elevation and log transformed gamma dose rates. The elevation explains 77.3% of the variation in gamma dose rate. The reason behind this is thought to be the fact that high areas are affected more from cosmic rays. The study area, Artvin has the roughest land in Artvin and changes in altitude are very fast. Correspondingly, sudden changes in gamma dose rates were identified in the study. Fig. 7a and b shows the relationship between gamma dose rates and elevation for both model data and test data, respectively. Great soil groups (GSG) explains 22.1% of the variation in gamma dose rate. The maximum of mean gamma dose rates were identified in high mountain meadow soils (Y) and the minimum was found in colluvial soils (C). Fig. 7c and d shows the box-and-whisker diagrams of gamma dose rates and great soil groups for both model data and test data, respectively.

From stepwise multiple linear regression (MLR) analysis, elevation, brown forest soils (M), non-calcic brown soils (N) and red–yellow podzolic soils (P) were significant ($p < 0.001$) variables in the MLR model [Eq. (13)] that explained 75.6% of the variability in Outdoor gamma dose rate (OGDR):

$$GDR = 2.071 + 0.0001(Elevation) - 0.262(M) - 0.499(N) - 0.178(P)$$
$$R^2 = 0.756 \quad (p < 0.001) \tag{13}$$

3.2. Geostatistical analysis

3.2.1. Spatial structure of gamma dose rate

Fig. 8a shows semivariogram surface that describes the spatial structure for gamma dose rate. Since this pattern is scattered homogenously to the whole area, spatial correlation was found to be nonanisotropic. Furthermore, as seen in the anisotropic experimental variogram, it can be concluded that the study area does not contain anisotrophy since the average variogram values are relatively close to each other in particular directions [0° (E–W), 45°(NE–SW), 90 (N–S) and 135 (diagonal)]. As a result of this, the area should be characterised with isotrophic semivariogram.

3.2.2. Variograms

OK interpolation can be specified with the formation of isotrophic experimental semivariogram and fitting of appropriate model to this variogram. UK interpolation is obtained with the forming of semivariogram of residuals in order to reidentify spatial structure with the help of proposed function according to MLR model given with equilibrium 13. In both of the experimental variograms, cross validation process is implemented in order to find the appropriate model and UK interpolated prediction can be made by using the obtained model parameters with fitted parametric function. Table 1 gives the summary of illustrative statistics that help us to choose the parametric model that best represents residual variogram.

For a model that ensures safe estimations, the mean error and the root mean square error should be close to 0 and the mean squared deviation ration should be close to 1. According to this, exponential model is specified as the best model both for outdoor

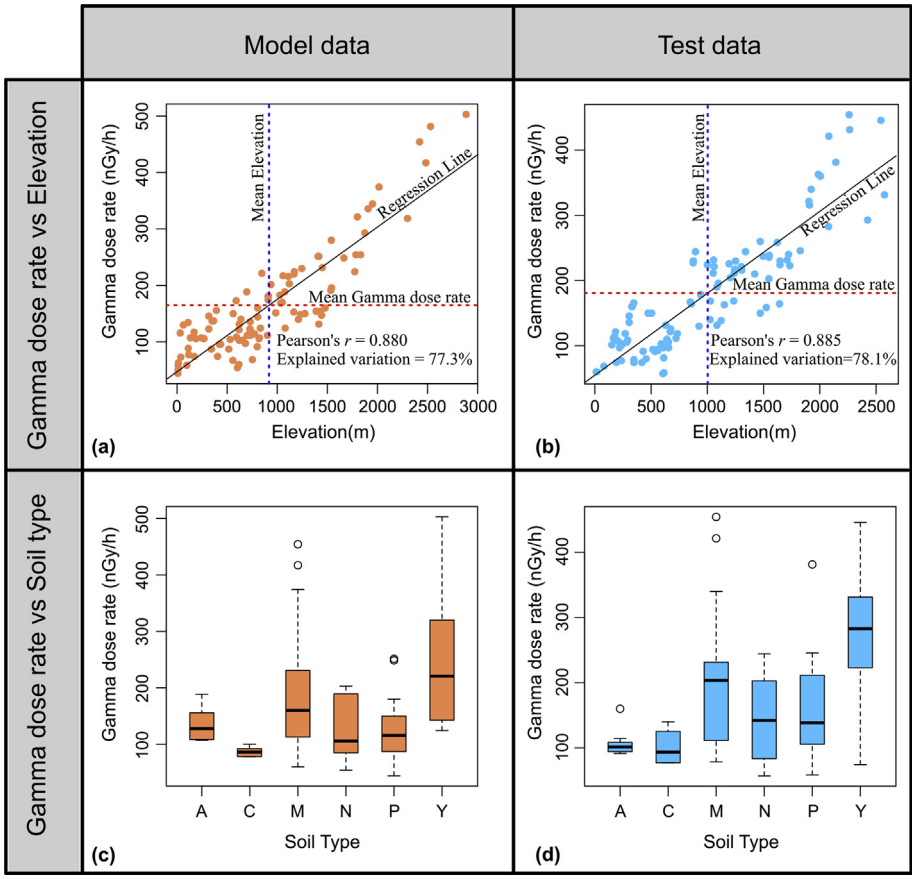

Fig. 7. Scatterplots showing the relation between gamma dose rate and elevation for (a) model data and (b) test data. Box-plots of gamma dose rate in nGy/h by great soil group for (c) model data and (d) test data.

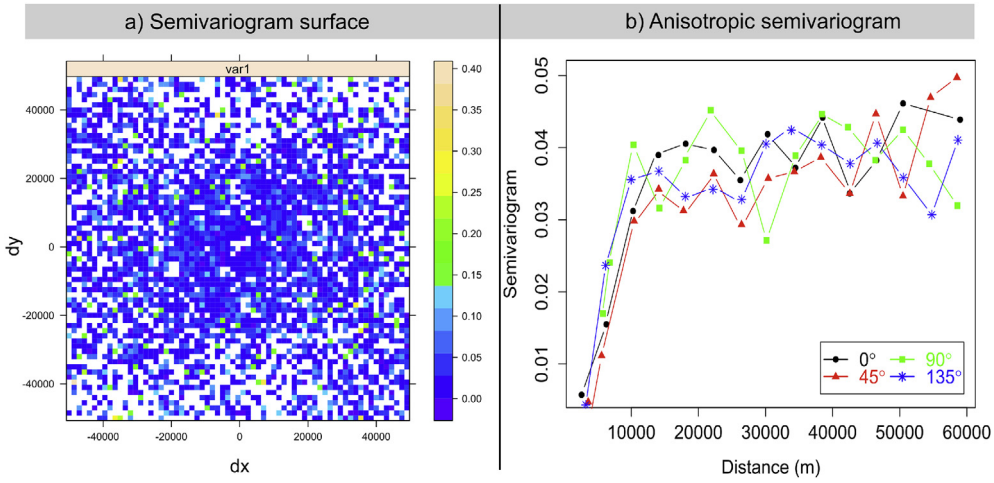

Fig. 8. Spatial structure of the study area (a) Semivariogram surface Gama dose rate, (b) Anisotropic variogram of gamma dose rates specified for particular directions.

gamma dose rates isotrophic experimental variogram and the regression residuals variogram. Fig. 9 shows these variograms and fitted model parameters. The nugget effect (C_0) is 0.001 and 0 for original variable (Fig. 9a) and MLR residuals variogram (Fig. 9b), respectively. These values are very small and show that the sampling density is adequate to reveal the spatial structures.

Furthermore, an indicator of spatial correlation, range (a) was specified as 7639.52 m and 4219.64 m, respectively. These values were quite bigger than sampling intervals (nearly 3000 m). Also, the nugget/sill ratio both in the variogram was less than 5% suggesting that the variable has strong spatial depence. As a result of these reasons, spatial structure that put forward the interpolation predicted maps was presented to represent gamma dose distribution best both in OK and UK.

3.2.3. *Validation*

Test data were predicted and by using ordinary kriging (OK) and universal kriging (UK) methods and making use of model parameters of fitted variograms with exponential models and these estimated test data were compared with the real values. Fig. 10 shows the scatter plot between the observed data and predicted data both for ordinary kriging and universal kriging. In estimation of OK and UK, 86.28% and 97.05% of the estimated points, respectively were inside the probability contour and there was a good linear relationship obtained between the real and estimated values. The cross validation has shown the average error of 4.7% for OK and 2.2% for UK. These results are quite small and can be used for estimation. In addition, the overall precision (RMSE) was calculated as 0.175 for OK and 0.093 for UK. Total variation in gamma dose rates suggested by using OK method was explained as 40.2% and Pearson r coefficient was found as 0.64 ($p < 0.001$). The total variation in gamma dose rates suggested by UK method was explained as 78.5% and Pearson r coefficient was found as 0.88 ($p < 0.001$).

Fig. 11 shows the diagnostic plots for observation and estimation regression with models formed by OK. Here, there was not any relationship found between the estimation values and residuals; that is to say, error values are statistically independent (Fig. 11a), error values show normal distribution (Fig. 11b) and probable distribution of error has constant variance (Fig. 11c). These results specify that estimation model done with OK fulfils the regression assumptions.

Fig. 12 shows the diagnostic plots for the observation regression and the estimation of the model formed with UK. Here, error values are statistically independent (Fig. 12a), error values show normal distribution (Fig. 12b) and error probability distribution has constant variance (Fig. 12c). According to these results, estimation model done with UK fulfils the regression assumptions.

With regard to these results, evaluating the two models in terms of performance, UK model was identified to be quite better than OK model in specifying the gamma dose rates spatially. Although OK model defines a specific amount of spatial correlation for gamma dose rates, because of the smoothing in the structure of kriging method, estimation values were below the average level and could not form a sufficient correlation with the real values (Fig. 10a). On the other hand, in the UK model generated by considering the trend components that directly affect gamma dose rates, smoothing had been partially reduced and there was a high correlation specified between estimation values and real values (Fig. 10b).

Table 1
The values of model parameters used to find the best fit function of semivariogram specified for original variable and regression residuals.

	Model	ME	RMSE	MSDR	Nugget	Sill	Range(m)	Nugget/Sill
Isotropic variogram for Gamma dose rate (log-scale)	Spherical	0.011	0.202	1.531	0.001	0.036	14,360.91	0.027
	Exponential	**0.008**	**0.186**	**1.253**	**0.001**	**0.040**	**7639.52**	**0.025**
	Gauss	0.012	0.213	3.078	0.001	0.036	6046.52	0.027
	Pentaspherical	0.010	0.201	1.497	0.002	0.036	17,784.57	0.055
	Linear	0.011	0.208	1.771	0.002	0.036	10,077.16	0.055
	Circular	0.011	0.205	1.586	0.002	0.036	12,215.91	0.055
Regression residuals variogram	Spherical	−0.003	0.112	1.470	0.0005	0.010	10,195.66	0.05
	Exponential	**−0.002**	**0.106**	**1.243**	**0.0000**	**0.010**	**4219.64**	**0.00**
	Gauss	−0.003	0.111	1.447	0.0020	0.008	5160.23	0.25
	Pentaspherical	−0.003	0.112	1.446	0.0001	0.010	11,929.92	0.01
	Linear	−0.003	0.112	1.451	0.0020	0.008	8991.44	0.25
	Circular	−0.003	0.111	1.402	0.0010	0.009	10,062.62	0.11

Fitted model are indicated with bold

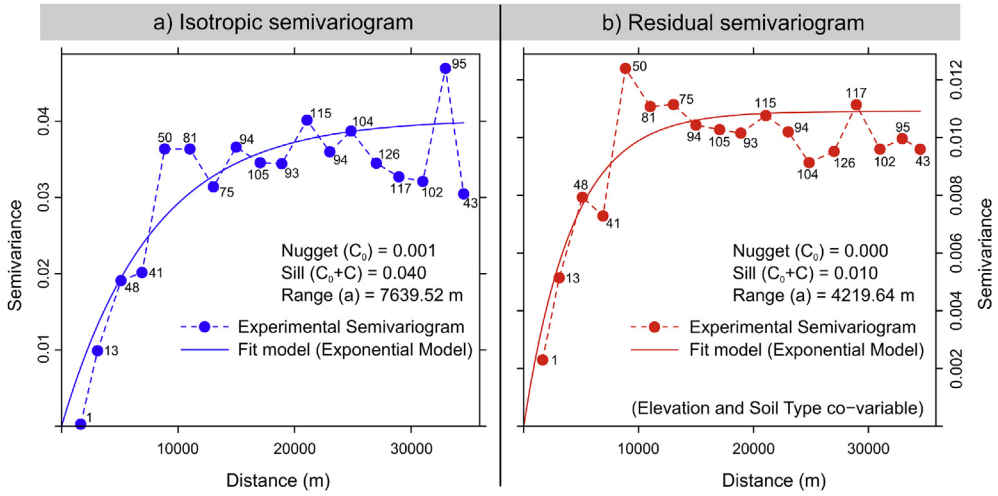

Fig. 9. a) Isotropic semivariogram for original variable (Log-scale), b) Residual semivariogram for MLR residuals. Numbers indicate total number of point pairs associated with each bin in the experimental semivariogram.

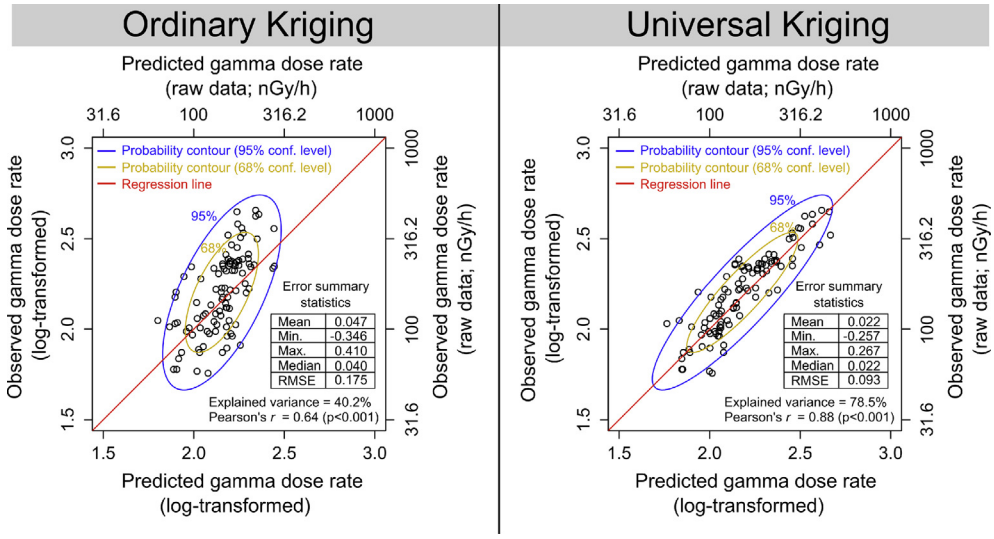

Fig. 10. The scatter diagram and error summary statistics of actual values of gamma dose rates versus obtained estimations by using OK and UK.

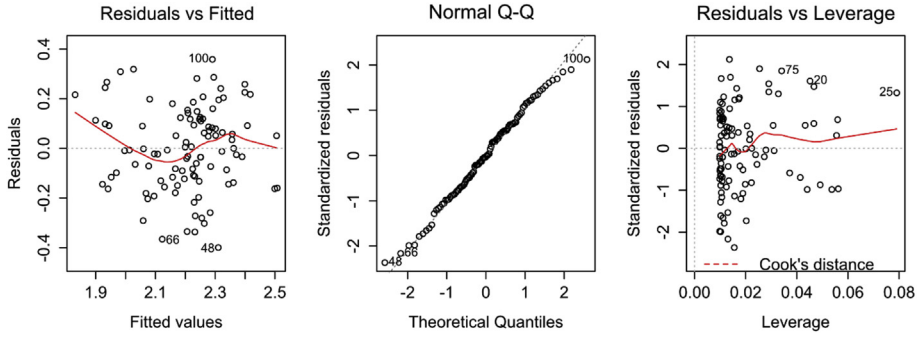

Fig. 11. Diagnostic plots for OK model.

3.2.4. Mapping

The study area was represented with grid system with separated cells of 100 m × 100 m (1 ha Spatial Resolution) in order to do the mapping and estimation of unsampling points. For the whole region, 1634 columns (E–W direction 163,400 m long) and 1409 lines (N–S direction 140,900 m long) were generated as grid points. Estimations were specified for both OK and UK methods in each grid point and maps were generated for each estimation method. Figs. 13 and 14 show OK interpolated prediction map and prediction variance of gamma dose rates, respectively. Although the local

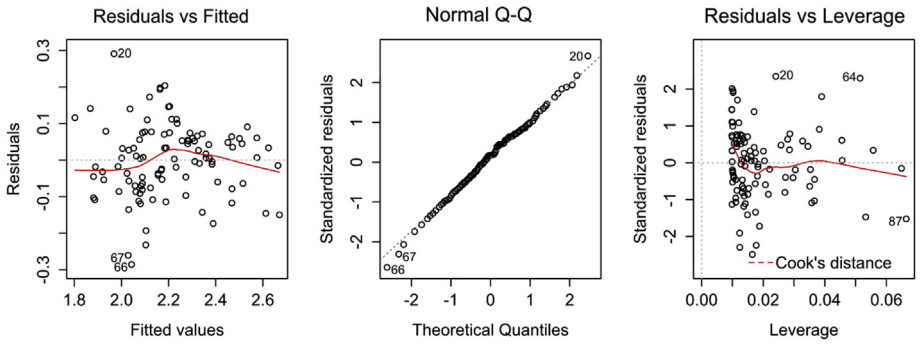

Fig. 12. Diagnostic plots for UK model.

changes are not seen clearly in the OK estimation map (Fig. 13) because of that smoothing effect of kriging method, gamma dose distribution in the study area can be defined. Gamma dose rates were found to be as low especially in the areas where the altitude is low (Black Sea coasts). Considering the study area together with geological (Fig. 3) and soil structure (Fig. 4), there was a significant increase in gamma dose rates especially in the places that have high mountain meadow soils group and granite structured rocks. OK estimation variance shown in Fig. 14 is associated with variogram structure and distribution of samples and provides the validity of kriging results (McGrath et al., 2004). This map shows the distribution of OK model maps. Here, estimation variance is very low in sampling sites that are close; however, this value is observed to be a little higher in far areas.

Figs. 15 and 16 show UK interpolated prediction map and estimation variance of gamma dose rates, respectively. In UK estimation map, smoothing effect of kriging method has been reduced. In the map generated using this model, local changes in gamma dose rates are more apparent. Rough study area and the sudden changes in altitude cause sudden changes in gamma dose rates and this situation is apparently shown in the map. In addition, in Fig. 15, it is identified that gamma dose rates are low along the basin of Çoruh River. UK estimation variance in Fig. 16 is relatively low. This is an indicator of low distribution in UK model errors and high validity levels of assigned results.

4. Conclusion

In this study, the distributions of gamma dose rates in Artvin, which possesses one of the roughest lands in Turkey, were studied, estimation values were calculated for non-sampling points by using the geostatistical model that best characterizes the region and the results were mapped. By doing so, with a specific measurement data, the general radiological structure of the study area was defined with minimum error. Ordinary kriging and universal kriging techniques were used in the study. In Universal kriging technique, both general soil groups and altitude values have been included as the estimators in the calculations. The data were normalized by log transformation because of the fact that the gamma dose rates in the study area did not show normal distribution. In order to reveal the spatial structure, anisotropic variograms were analysed and as a result, it was defined that these variograms did not change according to the directions. A good variogram structure was specified both for isotrophic and residual

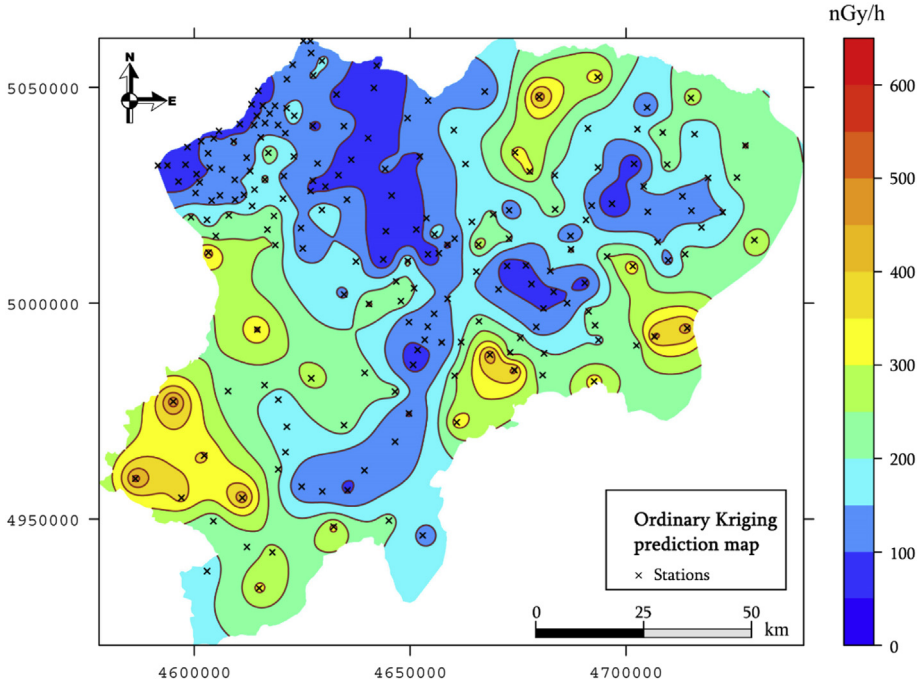

Fig. 13. OK interpolated estimation map for outdoor gamma dose rates.

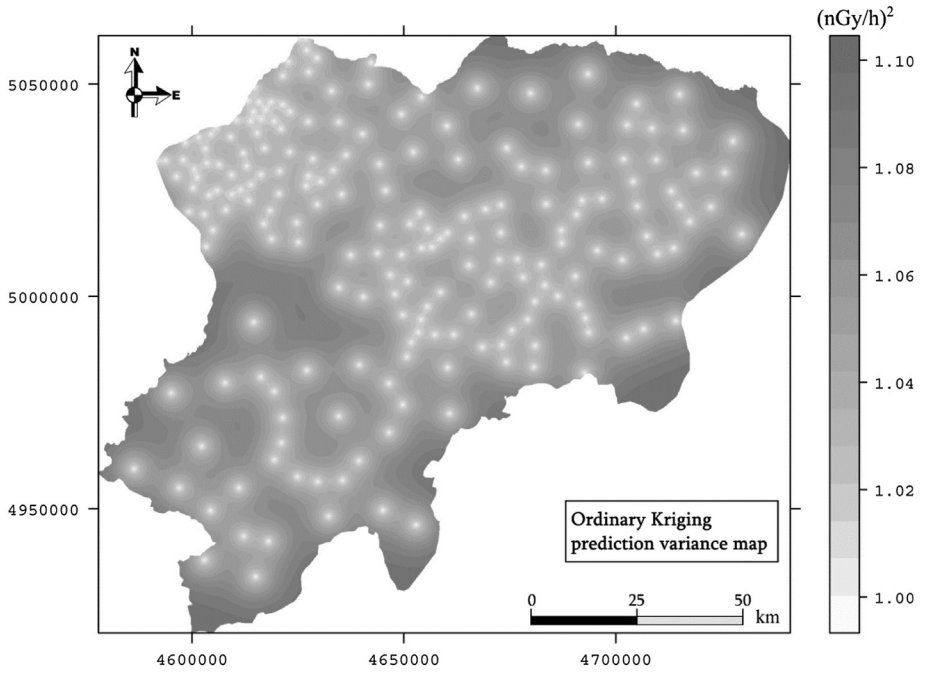

Fig. 14. OK estimation variance map for outdoor gamma dose rates.

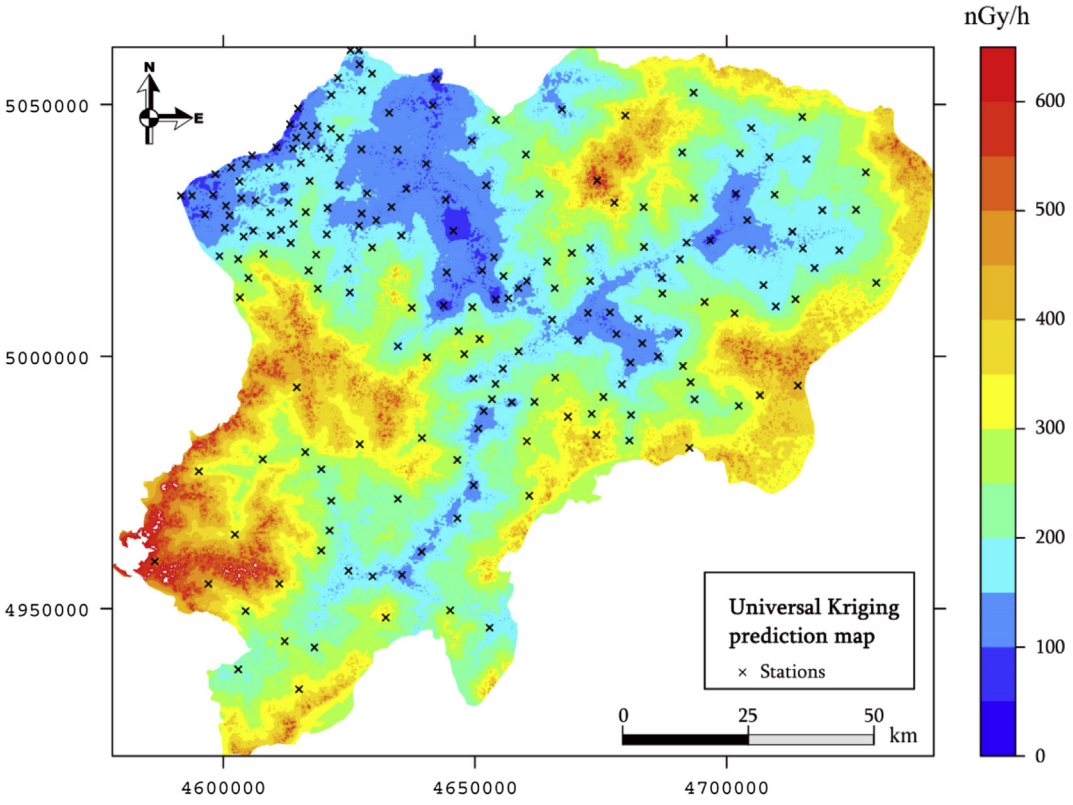

Fig. 15. UK interpolated estimation map for outdoor gamma dose rates.

variograms and both variograms were fitted the optimum parametric function, the exponential model. Thus, the necessary parameters for the weight calculations of Ordinary kriging and Universal kriging were identified with the help of fitted model. Validation was performed with the test data given to compare and contrast OK and UK methods. As a result, the variance defined with OK was found as 40.1% and Pearson's $r = 0.64$ ($p < 0.001$); however, the variance defined with UK was found to be 78.5% and Pearson's $r = 0.88$ ($p < 0.001$). The study area was divided into 100 m × 100 m (1 ha Spatial Resolution) cells for interpolated estimation maps and was represented with grid system. Estimation values were calculated for non-sampling parts by using both OK and UK methods and

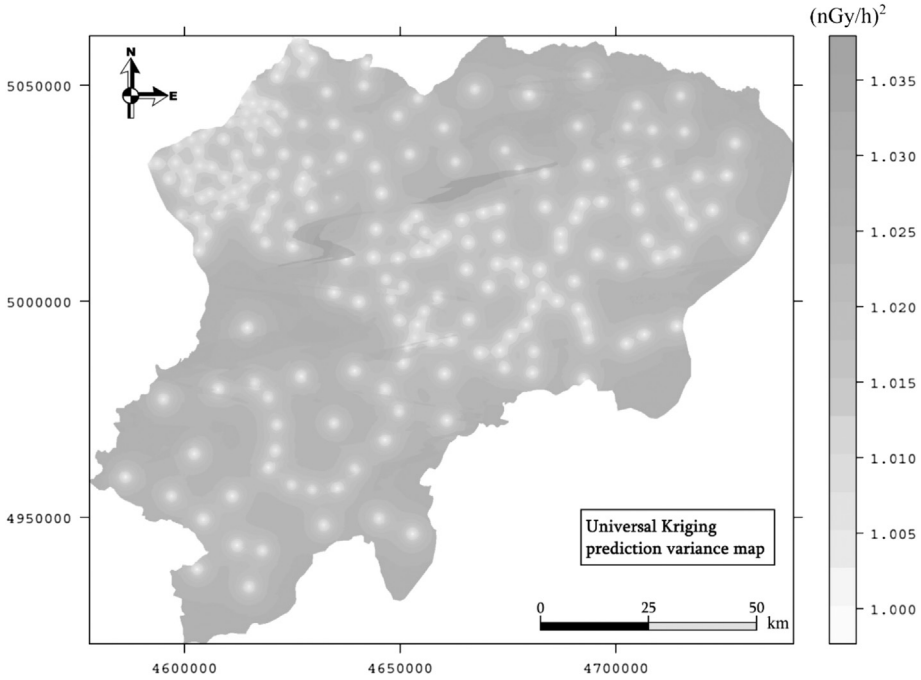

Fig. 16. UK estimation variance map for outdoor gamma dose rates.

maps were generated by colouring the grids according to this.

Although the map generated with OK model explained some parts of spatial correlation for outdoor gamma dose rates, the local changes in the study area could not be observed because of the smoothing done in the structure of the kriging method. However, in the UK model constructed by adding the factors like altitude and soil structure that directly affect gamma dose rates as estimators, smoothing effect was partially lowered and sudden changes in the study are were identified in the map. Thereby, in any routine or emergency case, Universal kriging method was established to perform better than Ordinary kriging in defining the radiological characterization of the land geostatistically with the least data in the shortest time.

Acknowledgements

This work was supported by Cekmece Nuclear Research and Training Centre (CNEAM) and Artvin Çoruh University research grant (BAP-2013.F42.02.05).

References

Alvarez-Gallego, M., Garcia-Anton, E., Fernandez-Cortes, A., Cuezva, S., Sanchez-Moral, S., 2015. High radon levels in subterranean environments: monitoring and technical criteria to ensure human safety (case of Castañar cave, Spain). J. Environ. Radioact. 145, 19–29. http://dx.doi.org/10.1016/j.jenvrad.2015.03.024.

Armstrong, M., 1998. In: Springer (Ed.), Basic Linear Geostatistics. Springer Science & Business Media, Berlin.

Baykara, O., Doğru, M., 2009. Determination of terrestrial gamma, U-238, Th-232 and K-40 in soil along fracture zones. Radiat. Meas 44, 116–121. http://dx.doi.org/10.1016/j.radmeas.2008.10.001.

Boogaart Van Den, K.G., Schaeben, H., 2002. Kriging of regionalized directions, axes, and orientations I. Directions and axes. Math. Geol. 34, 479–503.

Cafaro, C., Bossew, P., Giovani, C., Garavaglia, M., 2014. Definition of radon prone areas in Friuli Venezia Giulia region, Italy, using geostatistical tools. J. Environ. Radioact. 138, 208–219. http://dx.doi.org/10.1016/j.jenvrad.2014.09.003.

Charro, E., Pardo, R., Peña, V., 2013. Statistical analysis of the spatial distribution of radionuclides in soils around a coal-fired power plant in Spain. J. Environ. Radioact 124C, 84–92. http://dx.doi.org/10.1016/j.jenvrad.2013.04.011.

Chica-Olmo, M., Luque-Espinar, J.A., Rodriguez-Galiano, V., Pardo-Igúzquiza, E., Chica-Rivas, L., 2014. Categorical indicator Kriging for assessing the risk of groundwater nitrate pollution: the case of Vega de Granada aquifer (SE Spain). Sci. Total Environ. 470–471, 229–239. http://dx.doi.org/10.1016/j.scitotenv.2013.09.077.

Chilès, J.-P., Delfiner, P., 1999. In: Wiley (Ed.), Geostatistics: Modeling Spatial Uncertainty. Wiley, New York.

Clark, I., Harper, W.V., 2000. Practical Geostatistics 2000. Ecosse North America, ISBN 0-9703317-0-3. Columbus, Ohio, USA.

Chiozzi, P., Pasquale, V., Verdoya, M., 2002. Heat from radioactivite elements in Youngs volcanics by Gamma-Ray spectrometry. J. Volcanol. Geotherm. Res. 119, 205–214.

Clark, I., 1979. In: Elsevier (Ed.), Practical Geostatistics. Elsevier, London, U.K.

Dai, L., Wei, H., Wang, L., 2007. Spatial distribution and risk assessment of radionuclides in soils around a coal-fired power plant: a case study from the city of Baoji, China. Environ. Res. 104, 201–208. http://dx.doi.org/10.1016/j.envres.2006.11.005.

Degerlier, M., Karahan, G., Ozger, G., 2008. Radioactivity concentrations and dose assessment for soil samples around Adana, Turkey. J. Environ. Radioact. 99, 1018–1025. http://dx.doi.org/10.1016/j.jenvrad.2007.12.015.

Deutsch, C.V., Journel, A.G., 1998. In: Oxford Uni (Ed.), GSLIB: Geostatistical Software Library and User's Guide. Oxford University Press, New York.

Diggle, P., Riberioj, P., 2007. In: Springer (Ed.), Model-based Geostatistics. Springer, London, U.K.

Elbasiouny, H., Abowaly, M., Abu_Alkheir, A., Gad, A., 2014. Spatial variation of soil carbon and nitrogen pools by using ordinary Kriging method in an area of north Nile Delta, Egypt. CATENA 113, 70–78. http://dx.doi.org/10.1016/j.catena.2013.09.008.

Hiemstra, P.H., Pebesma, E.J., Twenhöfel, C.J.W., G.B.M., H., 2009. Real-time automatic interpolation of ambient gamma dose rates from the Dutch radioactivity monitoring network. Comput. Geosci. 35, 1711–1721. http://dx.doi.org/10.1016/j.cageo.2008.10.011.

Ihaka, R., Gentleman, R., 1996. R: a language for data analysis and graphics. J. Comput. Graph. Stat. 5, 299–314. http://dx.doi.org/10.1080/10618600.1996.10474713.

Karahan, G., Bayulken, a, 2000. Assessment of gamma dose rates around Istanbul (Turkey). J. Environ. Radioact 47, 213–221. http://dx.doi.org/10.1016/S0265-931X(99)00034-X.

Kobya Y., Taşkın H., Yeşilkanat, C.M. and Çevik U., Evaluation of outdoor gamma dose rate and cancer risk in artvin province, Turkey. Hum. Ecol. Risk Assess. Published online: 02 Mar 2015, http://dx.doi.org/10.1080/10807039.2015.1017876.

Krige, D.G., 1966. Two-dimensional weighted moving average trend surfaces for ore-evaluation. J. South Afr. Inst. Min. Met. 66, 13–38.

Lark, R.M., Ander, E.L., Cave, M.R., Knights, K.V., Glennon, M.M., Scanlon, R.P., 2014. Mapping trace element deficiency by cokriging from regional geochemical soil data: a case study on cobalt for grazing sheep in Ireland. Geoderma 226–227, 64–78. http://dx.doi.org/10.1016/j.geoderma.2014.03.002.

Li, C., Lu, Z., Ma, T., Zhu, X., 2009. A simple kriging method incorporating multiscale measurements in geochemical survey. J. Geochem. Explor. 101, 147–154. http://dx.doi.org/10.1016/j.gexplo.2008.06.003.

McGrath, D., Zhang, C., Carton, O.T., 2004. Geostatistical analyses and hazard

assessment on soil lead in Silvermines area. Irel. Environ. Pollut. 127, 239–248. http://dx.doi.org/10.1016/j.envpol.2003.07.002.
Mishev, A.L., Hristova, E., 2012. Recent gamma background measurements at high mountain altitude. J. Environ. Radioact. 113, 77–82. http://dx.doi.org/10.1016/j.jenvrad.2012.04.017.
MTA, 2002. 1:500 000–scale Map of Turkey. General Directorate of Mineral Research and Exploration (MTA), Ankara,Turkey.
Norbani, N.E., Abdullah Salim, N.A., Saat, A., Hamzah, Z., Ramli, A.T., Wan Idris, W.M.R., Jaafar, M.Z., Bradley, D. a., Abdul Rahman, A.T., 2014. Terrestrial gamma radiation dose rates (TGRD) from surface soil in Negeri Sembilan, Malaysia. Radiat. Phys. Chem. 104, 112–117. http://dx.doi.org/10.1016/j.radphyschem.2014.04.008.
O'Brien, K., Friedberg, W., Sauer, H.H., Smart, D.F., 1996. Atmospheric cosmic rays and solar energetic particles at aircraft altitudes. Environ. Int. 22, 9–44.
Otansev, P., Karahan, G., Kam, E., Barut, I., Taskin, H., 2012. Assessment of natural radioactivity concentrations and gamma dose rate levels in Kayseri. Turk. Radiat. Prot. Dosim. 148, 227–236.
Pebesma, E.J., 2005. Mapping radioactivity from monitoring data: Automating the classical geostatistical approach. Appl. GIS 1, 1–17. http://dx.doi.org/10.2104/ag050011.
Pebesma, E.J., Bivand, R.S., 2005. Classes and methods for spatial data in R. R. News 4, 9–13.
Pebesma, E.J., Wesseling, C.G., 1998. Gstat: a program for geostatistical modelling, prediction and simulation. Comput. Geosci. 24, 17–31. http://dx.doi.org/10.1016/S0098-3004(97)00082-4.
Quantum GIS Development Team, 2014. Quantum GIS Geographic Information System. Open Source Geospatial Foundation Project.
Quarto, M., Pugliese, M., Roca, V., 2013. Gamma dose rate measurements in dwellings of Campania region, South Italy. J. Environ. Radioact 115, 114–117. http://dx.doi.org/10.1016/j.jenvrad.2012.07.016.
Rafique, M., Rahman, S.U., Basharat, M., Aziz, W., Ahmad, I., Lone, K.A., Ahmad, K., 2014. Evaluation of excess life time cancer risk from gamma dose rates in Jhelum valley. J. Radiat. Res. Appl. Sci. 7, 29–35. http://dx.doi.org/10.1016/j.jrras.2013.11.005.
R Development Core Team, 2005. R: a Language and Environment for Statistical Computing, Reference Index Version 2.2.1 [WWW Document]. R Found. Stat. Comput. URL. http://www.r-project.org/.
Ramasamy, V., Paramasivam, K., Suresh, G., Jose, M.T., 2014. Role of sediment characteristics on natural radiation level of the Vaigai river sediment, Tamil-nadu, India. J. Environ. Radioact. 127, 64–74. http://dx.doi.org/10.1016/j.jenvrad.2013.09.010.
Sanusi, M.S.M., Ramli, A.T., Gabdo, H.T., Garba, N.N., Heryanshah, A., Wagiran, H., Said, M.N., 2014. Isodose mapping of terrestrial gamma radiation dose rate of Selangor state, Kuala Lumpur and Putrajaya, Malaysia. J. Environ. Radioact. 135, 67–74. http://dx.doi.org/10.1016/j.jenvrad.2014.04.004.
Savelieva, E., 2005. Using ordinary Kriging to model radioactive contamination data. Appl. GIS 1, 10-1-10-10.
Statistic Department of Turkey, 2014. http://www.webcitation.org/6NPUa8fse. Available date: 08.09.2014.
Taskin, H., Karavus, M., Ay, P., Topuzoglu, a, Hidiroglu, S., Karahan, G., 2009. Radionuclide concentrations in soil and lifetime cancer risk due to gamma radioactivity in Kirklareli, Turkey. J. Environ. Radioact. 100, 49–53. http://dx.doi.org/10.1016/j.jenvrad.2008.10.012.
Tondel, M., Lindgren, P., Hellström, L., Löfman, O., Fredrikson, M., 2011. Risk of malignancies in relation to terrestrial gamma radiation in a Swedish population cohort. Sci. Total Environ 409, 471–477. http://dx.doi.org/10.1016/j.scitotenv.2010.10.052.
UNSCEAR, 2000. Source and effects of ionizing radiation, United Nations Scientific Committee on the Effects of Atomic Radiation. United Nations, New York.
USGS, 2013. Digital Elevation Maps (DEM) Data Sets (Available date: 11.01.2015) [WWW Document]. URL. http://earthexplorer.usgs.gov/. http://earthexplorer.usgs.gov/.
Ustaomer, T., Robertson, a. H.F., Ustaomer, P. a., Gerdes, a., Peytcheva, I., 2012. Constraints on Variscan and Cimmerian magmatism and metamorphism in the Pontides (Yusufeli-Artvin area), NE Turkey from U-Pb dating and granite geochemistry. Geol. Soc. Lond. Spec. Publ. 372, 49–74. http://dx.doi.org/10.1144/SP372.13.
Warnery, E., Ielsch, G., Lajaunie, C., Cale, E., Wackernagel, H., Debayle, C., Guillevic, J., 2015. Indoor terrestrial gamma dose rate mapping in France: a case study using two different geostatistical models. J. Environ. Radioact. 139, 140–148. http://dx.doi.org/10.1016/j.jenvrad.2014.10.002.
Webster, R., Oliver, M.A., 2007. Geostatistics for Environmental Scientists. Wiley. John Wiley & Sons.
Yavuz Özalp, A., Akıncı, H., Temuçin, S., 2013. Determining topographic and some physical characteristics of the land in artvin City and investigating relationship between these characteristics with land cover. J. For. Fac. Artvin Coruh Univ. 14, 292–309.
Yuksek, T., Ölmez, Z., 2002. A general assessment of climate, soil structure, forest areas, growing stock and some forestry applications of Artvin region. J. Artvin For. Fac. Kafkas Univ. 3, 50–62.